Factors influencing chloride deposition in a coastal hilly area and application to chloride deposition mapping

Huade Guan[1,2], Andrew J. Love[1,3], Craig T. Simmons[1,2], Ahmet S. Kayaalp[4], Oleg Makhnin[5]

1. School of Chemistry, Physics and Earth Sciences, Flinders University, Australia

2. National Centre for Groundwater Research and Training, Australia

3. Department of Land, Water, and Biodiversity Conservation, South Australia

4. Water Technology Division, Water Corporation, West Australia

5. Department of Mathematics, New Mexico Institute of Mining and Technology, U.S.A.

Contact:

Dr. Huade Guan, School of Chemistry, Physics & Earth Sciences, Flinders University, Australia, +61 8 82012319, huade.guan@flinders.edu.au

Abstract

Chloride is commonly used as an environmental tracer for studying water flow and solute transport in the environment. It is especially useful for estimating groundwater recharge based on the commonly used chloride mass balance (CMB) method. Strong spatial variability in chloride deposition in coastal areas is one difficulty encountered in appropriately applying the method. A high resolution chloride deposition map in the coastal region is thus needed. The aim of this study is to construct chloride deposition map in the Mount Lofty Ranges (MLR), a coastal hilly area of approximately 9000 km^2 spatial extent in South Australia. We examined geographic, orographic, and atmospheric factors influencing chloride deposition, using partial correlation and regression analyses. The results indicate that coastal distance, and terrain aspect and slope are two most significant factors controlling chloride deposition in the study area. Coastal distance accounts for 65% spatial variability in chloride deposition, with terrain aspect and slope for 8%. The average deposition gradient is about 0.08 $gm^{-2}year^{-1}km^{-1}$ as one progresses inland. The results are incorporated into a published de-trended residual kriging approach (ASOADeK) to produce a 1 km × 1 km resolution bulk chloride deposition and concentration maps. The average uncertainty of the deposition map is about 20% in the western MLR, and over 50% in the eastern MLR. The maps will form a very useful basis for examining catchment chloride balances for use in the CMB application in the study area.

Key words

Chloride deposition, orographic effect, chloride mass balance, kriging, multivariate regression, partial correlation

1. Introduction

Chloride is commonly used as an environmental tracer for studying water flow and solute transport in surface water bodies (Dunn and Bacon, 2008; Shaw et al., 2008; Hrachowitz et al., 2009), vadose zones and aquifers (Eriksson and Khunakasem, 1969; Walker et al., 1991; Cook et al., 1992; Phillips, 1994; Wood and Sanford, 1995; Kirchner et al., 2000; Edmunds et al., 2002; Scanlon et al., 2002; Minor et al., 2007). It is especially useful to estimate groundwater recharge based on chloride mass balance (CMB). The CMB method can be applied either for estimating point recharge with chloride concentration in the steady-state soil profile, or for estimating catchment-average recharge with chloride concentration in mean groundwater. For situations that the atmospheric input is the only chloride source, and that no chloride sinks exist in the system, the CMB method can be formulated as

$$C_p P = C_g G + C_r R \qquad (1)$$

where C_p is chloride concentration in bulk precipitation, P is average precipitation, C_g is chloride concentration in the soil water far below the root zone or in groundwater that was recharged from the catchment, G is groundwater or soil water that is equilibrium with the surface conditions, C_r is chloride concentration in the runoff R. The CMB method does not require knowledge of dynamic hydrological processes (although with such information, it would help to apply the CMB method more reliably). Thus, the method provides a good solution to estimate groundwater recharge in mountainous terrain where hydrogeological and hydrometeorological conditions are complex (Wilson and Guan, 2004). In order to apply the CMB method, the atmospheric chloride input must be known. In the inland area, atmospheric chloride deposition does not change much over a large distance (e.g., ~100 km) (Keywood et al., 1997). One estimate of average chloride deposition either directly from bulk precipitation sampling, or inferred from the ratio of ^{36}Cl/Cl which has a 30% uncertainty (Scanlon, 2000), is often used in the CMB calculation. In the coastal area, however, large spatial variability of chloride deposition is often observed (Blackburn and McLeod, 1983; Keywood et al., 1997; Kayaalp, 2001; Biggs, 2006; Alcala and Custodio, 2008a). A detailed map of atmospheric chloride deposition is thus needed to apply the CMB approach for estimating groundwater recharge in the coastal areas.

It is commonly accepted that the primary source of the atmospheric chloride is from the ocean by wind-induced whitecaps and bursts, which inject sea water drops into the atmosphere (Lewis and Schwartz, 2004). About 10% of total chloride in the sea salt aerosols moves into the continents, and the majority of this chloride is deposited within 100 km of the coastal area (Eriksson, 1959; Eriksson, 1960). It should be noted that the anthropogenic sources may add chloride to the atmosphere at some extreme situations where air pollution is serious (Alcala and Custodio, 2008b). Two primary mechanisms, dry deposition and wet deposition, control chloride removal from the atmosphere to the land surface. Chloride-bearing aerosols can settle down to the surface by gravitational forces. This dry deposition process is highly dependent on wind conditions and the aerosol size. Chloride in the aerosols can also be rained out from the cloud, or washed out by the falling rain drops. This wet deposition process is dependent on precipitation characteristics. In terms of hydrological applications, it is the total chloride deposition (bulk chloride deposition, or BCD hereafter), i.e., the sum of wet and dry depositions, that is important because it gives the input chloride for the CMB calculation (Wood and Sanford, 1995). Thus, BCD is usually measured from accumulated rain samples over a certain period, with samplers sitting in an open area, and open to the sky all the time. As chloride-bearing aerosols originate from the ocean, it is typically observed that BCD over the continents decays exponentially with increasing distance from the coast (coastal distance hereafter) (Keywood et al., 1997; Gustafsson and Larsson, 2000). Over a short distance, linear relationship can be used to approximate the change of BCD with coastal distance (Alcala and Custodio, 2008a). The relationship between elevation and BCD has been implicitly shown, but not conclusive remark is made as the other effect such as coastal distance was not separated (Contreras et al., 2008).

This coastal distance dependence, when quantitatively determined, is useful to estimate BCD for a point location at some known distance from the coast. However, deposition processes are also associated with the prevailing wind direction and it is therefore difficult to use the distance-dependence function alone to construct good resolution BCD maps. Instead, kriging is frequently used to map BCD. Carratala et al. (1998) performed ordinary kriging with 28 data points to construct 10 km × 15 km resolution bulk chloride concentration map on the eastern coast of Spain. Gustafsson and Larsson (2000) applied ordinary block kriging to construct 10 km × 10 km resolution seasonal BCD maps with 49 data points over an area of 8×10^4 km^2 in southern Sweden. Alcala and Custodio (2008a) used ordinary kriging to produce 10 km × 10 km mean annual BCD map with measurements over 200 geographic points for continental Spain (5×10^5 km^2). The ratio of data points over mapping pixels of the above three mapping exercises ranges from one 16th to about one 60th. In the coastal area, BCD often varies significantly even over a few kilometres (Kayaalp, 2001). The aim of this study is to construct BCD map at a spatial resolution of 1 km × 1 km over an area of 9000 km^2, based on 17 data points. In contrast to earlier mapping studies, the ratio of data points over mapping pixels in this study is only one 500th. The sparse data points and small sample size largely increase uncertainty of the kriging estimates (Chang et al., 1998). Can we incorporate some associated physical process information, including coastal distance dependence, so as to make more reliable estimates for chloride deposition to form a basis for BCD mapping? In this context, geostatistical approaches, such as residual kriging (RK), kriging with external drift (KED), and cokriging (CK), can be used to incorporate secondary variable information in the mapping (Isaaks and Srivastava, 1989; Goovaerts, 2000; Guan et al., 2005). Because of the difficulty to select appropriate secondary variables and functions, RK is chosen, in which the secondary variable effect, often called trend estimate, is determined first (Isaaks and Srivastava, 1989, p532). Similar approach has been successfully applied in precipitation and rain water isotope mapping in mountainous terrains (Guan et al., 2005; Guan et al., 2009). The objectives of this study are first to examine the influencing factors associated with physical processes that control chloride deposition by correlation and regression analyses, and based on this to construct BCD map by RK.

The study is based on Adelaide and the Mount Lofty Ranges (MLR) of South Australia. The whole area has 1.2 million residents, with 60% water supply coming from on the MLR. A reliable BCD map is important for water resources management over the region. To understand the influencing factors on BCD in the study area, our starting hypotheses are that in addition to coastal distance, (1) windward slopes, associated with sea breeze and in-coming moisture direction, enhance BCD due to topographic interception, and orographic precipitation, and (2) elevation enhances BCD due to increasing precipitation. Although vegetation canopy may influence BCD (Moreno et al., 2001), as bulk chloride samples used in this study were collected in the open area, the canopy effect is not accessed. The results indicate that terrain slope and aspect (slope orientation), associated with prevailing wind direction, may influence BCD in the coastal area, but in a manner that is contrary to our starting hypothesis. The elevation does not significantly affect BCD. These results are helpful to improve our understanding of sea salt deposition in the coastal area. These new findings are incorporated into BCD mapping for the study area. The mapping result is compared to ordinary kriging estimates, and cross validated with the observation data. The chloride map produced here will be used to examine the catchment chloride balance status, which is to be discussed in a subsequent paper.

2. Methodology

2.1 Study area and data

The study area lies in and to the east of Adelaide, South Australia (Fig. 1). It covers an area of about 9000 km^2, with topographic relief of 700 m. To the west is Gulf St Vincent, which extends about 150 km long and 70 km wide. To the south is the Southern Ocean, with saline lake Alexandria sitting to the southwest. The primary industries include health service, education, winery and agriculture. No obvious air pollution sources of chlorine exist in the area. The bedrock in the MLR is primarily late Precambrian metamorphous sedimentary rock composed of shale and sandstone, and some limestone (Preiss, 1987). The climate is of Mediterranean type, with wet winters and dry summers. The annual precipitation ranges from below 300 mm to above 1000 mm, with an areal average of 600 mm (Guan et al., 2009). Mean daily temperature over the area is about 15-18°C. The annual pan evaporation at a location of 600-mm precipitation (about area-average value) is about 1500 mm (BOM, 2009). Prevailing westerly moisture flux feeds precipitation (Guan et al., 2009), and thus wet chloride deposition in the area. Westerly sea breezes occur frequently during part of the day (Fig. 2, and later Fig. 9) over most of the study area, which fuel atmospheric transport of sea salt aerosols from the Gulf St Vincent and facilitate dry deposition. At the south edge of the area, no dominant southerly wind is observed. Thus, from both wet and dry deposition points of view, dominant atmospheric chloride source in this area is from the west.

Bulk chloride concentration was measured at 17 sites in the open area, over two periods by two organizations: Flinders University (1992-1994) and Department of Water, Land and Biodiversity Conservation (DWLBC) (2002-2005) (Table 1). It is BCD in the open area that is examined in this study. Although canopy may change chloride deposition rates, its effect is difficult to evaluate because this information is not included in our samples. DWLBC samples were multiple-month cumulative rain, while Flinders samples were collected daily and summed to monthly. For DWLBC sampling, following common procedure (Friedman et al., 1992), a thin layer of mineral oil was applied in the collectors to avoid water evaporation over the two sampling periods. On average the sampling duration is about 2 years, with two sites (Sites 4 and 5) sampled for shorter than one year. They are nevertheless included because the sampling period covers both halves of the dry and rainy seasons. Both rain sample volume and chloride concentration were measured for each cumulative sample. Chloride concentration was measured with an ion chromatography system, with standard deviation of repeat testings less than 0.1 mg/l over the normal sample concentration range, at Land and Water Division of the Commonwealth Scientific and Industrial Research Organization, Adelaide, Australia. Average chloride concentrations and annual chloride deposition are calculated from samples at each of the 17 sites (Table 1). In addition, wind direction data for 41 sites in and near the study area were obtained from the Bureau of Meteorology of Australia (BOM) (Fig. 1). Wind direction was recorded twice daily at 9:00AM and 3:00PM local time.

2.2 Correlation analysis

Correlation analysis has been widely used to examine linear association between variables. The Pearson product-moment correlation coefficient (*r*) is the most common measure of linear association between two variables. When multiple variables are correlated to one another, the correlation coefficient of the variable of interest with any one of the other variables may give association implication which is not physically dependent. To solve this problem, a partial correlation coefficient is applied to examine the linear correlation between the two variables with the effects of other selected variables removed (Lowry, 1999-2009). An example of partial correlation coefficient between variables x and y independent of a third variable (z) is calculated using

$$r_{xy(z)} = \frac{r_{xy} - r_{xz} r_{yz}}{\sqrt{1 - r_{xz}^2}\sqrt{1 - r_{yz}^2}} \qquad (2)$$

where r is Pearson correlation coefficient between the two variables denoted in the subscripts. The partial correlation coefficients are calculated with MATLAB in this study. After $r_{xy(z)}$ is obtained, the significance is tested with a t-distribution. The t-value is calculated by

$$t = \frac{r_{xy(z)}}{\sqrt{(1 - r^2)/(N - 2)}} \qquad (3)$$

where N (≥ 6) is the number of samples (Lowry, 1999-2009). Strictly speaking, the significance testing relies on the assumption that each variable is spatially independent, which is often invalid for regionalized random variables, such as the ones examined here. Thus, the p-values from the correlation analysis are not strictly correct. Nevertheless, they should be still useful to compare which variables are more important than others to be associated with chloride deposition, and to determine which variables are not significant (details are discussed in the Results section). This loose significance test is applied to examine our two hypotheses, one relating to the elevation effect and the other relating to terrain aspect (slope orientation) effect on BCD. If the tested factor is important in BCD, the partial correlation coefficient between BCD and the factor variable should have a corresponding *p* values much smaller than others.

2.3 ASOADeK regression and mapping

A multivariate regression embedded in a geostatistical model (Auto-searched Orographic and Atmospheric effects De-trended Kriging, or ASOADeK) has been shown to successfully capture geographic and orographic effects on precipitation distribution over mountain terrains (Guan et al., 2005). The ASOADeK model has two components: a regression to obtain the trend estimates, and a residual kriging to compensate where the regression estimate is poor. The regression was originally developed to auto-search the effects of atmospheric moisture gradient, prevailing moisture flux direction associated terrain aspect and slope, and terrain elevation, on precipitation distribution. Recently, it was applied to examine orographic effects on rain isotope distribution (Guan et al., 2009). Since wet deposition occurs with precipitation, and dry deposition over the area has similar westerly source as precipitation, we attempt to use the ASOADeK regression to examine the effects of selected geographic and topographic variables on BCD. The original regression model, including both elevation and terrain aspect, can be found in (Guan et al., 2005). The regression model used below including elevation, terrain aspect and slope, first appears in (Guan et al., 2009).

$$D = b_0 + b_1 X + b_2 Y + b_3 Z + b_4 \beta \cos\alpha + b_5 \beta \sin\alpha \quad (4)$$

where D is annual BCD (gm^{-2}), X and Y are geographic coordinates (usually as easting and northing in the Universal Transverse Mercator (UTM) coordinate system, in km), used to capture the effect of coastal distance dependence, Z is above-sea-level terrain elevation in kilometres, β is the slope angle in degree, α is the terrain aspect, defined as the direction of slope orientation, zero to the north, increasing clockwise, and 180 to the south. The two trigonometric terms are derived from $\cos(\alpha - \omega)$, where ω is the source flux direction. This function has a value of 1 at windward slopes, and -1 at leeward slopes. This formulation was originally designed to capture the orographic effect of more precipitation (or chloride deposition) on the windward slope than on the leeward side. If chloride deposition is enhanced in the leeward side, the sign of b_4 and b_5 will be reversed. For situations where the sample size is small, only the terms of statistical significance should be included in the regression. As discussed later, only two predictor variables are applied for BCD distribution in the study area.

After regression is performed, it is used to generate a regression estimate map (the trend) based on a DEM. The difference between the observations and regression estimates are then used to generate a de-trended residual map by ordinary kriging. The final BCD map is the sum of the regression map and the residual map. This procedure is simply called ASOADeK mapping. More details of this approach can be found in (Guan et al., 2005). The performance of this mapping approach is examined by cross validation, in which each of the total N data points is set aside each time to compare with the mapping estimate at the location based on the remaining (N-1) data points (Isaaks and Srivastava, 1989). Both regression and semivariogram modeling are performed for each cross validation set. The mapping result is also compared to direct ordinary kriging of the observed chloride depositions. This is called direct kriging, to be distinguished from the residual kriging, which is one component of ASOADeK model. All kriging calculations are performed with Geostatistical Software Library (Deutsch and Journel, 1998). Finally, the bulk chloride concentration map is then constructed based on the annual chloride deposition map and annual precipitation map of the study area, both at a spatial resolution of 1 km × 1 km.

After the ASOADeK mapping, the uncertainty originated from the mapping approach is calculated. The mapping uncertainty (ε) is composed of the regression uncertainty and residual kriging uncertainty. With an assumption that the mapping uncertainty follows normal distribution, it is calculated as

$$\varepsilon = u\sqrt{{\varepsilon_r}^2 + V_k} \tag{5}$$

where u is the critical value of the standard normal distribution, (1.645 for 90%, and 1.960 for 95% confidence level), ε_r is the standard error of the regression fit, and V_k is kriging variance. A confidence level of 90% is used in this study.

3. Results

3.1 Correlation analysis and hypothesis testing

As discussed in 2.1, both wet and dry deposition in the study area tend to come from a westerly direction. Chloride deposition data of most of the 17 sites (Table 1, Fig. 3) follows this trend. However, at sites 16 and 17, chloride deposition is abnormally high in comparison to site 15. Thus, sites 16 and 17 are excluded from correlation and regression analysis, to avoid their anomalous disturbance on investigating the physical processes common to the whole area. However, sites 16 and 17 are included for residual kriging and to generate the chloride deposition map. Although an exponential decrease in bulk chloride deposition (D) with increasing coastal distance (approximately X in the study area) is reported at a large scale (Keywood et al., 1997; Gustafsson and Larsson, 2000), a linear relationship is observed between D and X in the study area with coastal distance within 100 km (Fig. 3). This feature supports that a linear correlation and regression analyses between D and X is appropriate over the spatial scale of the study area.

With sites 16 and 17 excluded, the correlation matrix of chloride deposition with precipitation and five selected variables is included in Table 2. Based on a one-tailed t test, $|r|$ needs to be 0.44 for a significant level of p = 0.05, and 0.35 for p = 0.10 given a sample size of 15 (Lowry, 1999-2009). Because of spatial dependence of the examined variables, the significant threshold $|r|$ should be larger than the above values at each confidence level, but the exact line is difficult to define. Nevertheless, these values are useful to determine which variables are not significantly associated with D. For example, based on the r values, Z and $\beta \cos \alpha$ are not significantly correlated to D. The r and p values should be also useful to evaluate relative significance of linear association between D and each of the other examined variables. D and X (easting) have the highest negative correlation. This is consistent with the westerly chloride source for the study area and coastal distance-dependent chloride deposition reported in the literature. The r values suggest that P (precipitation) is correlated with D, but also with X. Y (northing) and $\beta \sin \alpha$ are both correlated with X. Based on the correlation matrix, it is difficult to evaluate the association of P, Y , and $\beta \sin \alpha$ with D. Partial correlation coefficients (Fig. 4), with the effect of X removed, suggest that Y and P are not significantly associated with D. The relative significance test indicates that $\beta \sin \alpha$ is the second significant term, next to X, correlated with D. This implies that slope and aspect may affect BCD. With *X* and *P* effect removed, the correlation between *D* and $\beta \sin \alpha$ is similar to that with *X* effect removed, suggesting that dry deposition may be affected by terrain aspect and slope. With precipitation effect removed, partial correlation coefficient between *D* and *X* is -0.76, suggesting that dry deposition has a similar coastal-distance dependence as BCD. Partial correlation analysis results confirm the insignificant association between *D* and *Z*, and between *D* and $\beta \cos \alpha$.

We now examine the two hypotheses, (1) elevation and (2) west-facing slope facilitating chloride deposition, as they pertain to possible topographic influences on chloride deposition. Elevation apparently does not enhance chloride deposition, as no significant linear association is found from either the correlation matrix or the partial correlation analysis. Terrain aspect and slope are the second significant factor, next to the coastal distance, for BCD in the study area, as indicated by the partial correlation between *D* and $\beta \sin \alpha$. The partial correlation coefficient between the two variables is positive. Based on the definition of terrain aspect α in Eq. (4), it has a positive value on east-facing slopes. This indicates that more chloride deposition occurs on eastern slopes (leeward slopes in respect to the atmospheric chloride source direction, instead of on the western (windward) slopes in our starting hypothesis.

3.2 Regression analysis and ASOADeK mapping

Based on partial correlation analysis, among the five predictor variables in Eq. (4), the two most significantly linearly associated factors to BCD are *X* and $\beta \sin \alpha$. Thus, regression is performed with *X* and $\beta \sin \alpha$ only (Table 3). The results indicate that coastal distance explains about 65% of the spatial variability in chloride deposition in the study area, while terrain aspect accounts for an additional 8%. Based on the regression results, the chloride deposition gradient average over the study area is about 0.08 $gm^{-2}year^{-1}km^{-1}$ downwind away from the coast. This value is within the range of 0.05 to 0.25 $gm^{-2}year^{-1}km^{-1}$ reported for Spain's non-polluted Mediterranean coastal areas (Alcala and Custodio, 2008a).

After regression is performed, it can be used to construct the BCD regression map and ASOADeK map. To examine the mapping performance, cross validation was performed in comparison to the direct ordinary kriging. One example of cross-validation semivariogram model for direct kriging is shown in Fig. 5a. It is similar among 17 sets of cross-validation data. The semivariagram models for cross-validation residual sets are not shown, as they are different among the 15 sets. In comparison to direct kriging, both regression and ASOADeK estimates give a smaller mean absolute error (MAE), calculated from all cross-validation sets, and higher correlation coefficient between the estimates and observations (Fig. 6a). The MAE value of regression cross validation is 0.80 g/m^2, about 20% of average observation values over the first 15 locations in Table 1, and the MAE value of ASOADeK cross validation is 0.84 g/m^2, about 21% of the observation average. ASOADeK cross validation results slightly degrades in comparison to that of the regression, probably because the chloride network density is too low. The residual kriging is nevertheless applied because sites 16 and 17 were not included in the regression.

Comparison of cross validations provides us confidence to construct BCD map using the ASOADeK method. The various maps derived from ASOADeK mapping approach are included in Fig. 7a-d. The regression map (Fig. 7a) primarily shows the coastal distance and terrain aspect and slope effects. It underestimates chloride deposition in the southeastern corner of the area, because the two data points (16 and 17 in Table 1) were not included in the regression. The residual kriging is performed with the semivariogram model shown in Fig. 5b. The regression underestimates in the southeastern corner are compensated by large positive residuals (Fig. 7b). The chloride deposition map (Fig. 7c) is constructed as the sum of regression and residual maps. Overall, annual chloride deposition rate is over 6 gm^{-2} in the southwestern corner and western coast, decreasing to 4-5 gm^{-2} in the central part, and to below 2 gm^{-2} in the eastern and northeastern edges of the area. The mapping uncertainty is calculated based on Eq. (5) and shown in Figure 7d, with BCD observation sites included for comparison. The average uncertainty in the western half is some 1 gm^{-2}, about 20% of the estimated chloride deposition, while in the eastern half, average uncertainty is over 1.5 gm^{-2}, about 50% of the estimated chloride deposition (Fig. 7d). This value is similar or larger than the cross-validation MAE values. The uncertainty at the sampling sites is small. The mean absolute error of the regression estimates at the 15 sites is 0.54 gm^{-2}, equivalent to 14% of the average observed annual chloride deposition at these sites (Table 3) (Fig. 6b). After the residual kriging is added, the mean absolute error over the 17 sites is reduced to 0.41 gm^{-2} (Figure 6b, this is different from cross validation results shown in Figure 6a), about 11% of the average observed annual deposition at these sites. A long term mean precipitation map was previously constructed for the study area, based on a much denser observation network (96 gauges) and a much longer observation period (the majority of these data have over 30 years record) (Guan et al., 2009). The average uncertainty of the precipitation map is about

2% at 90% confidence level. Based on this, and the chloride deposition maps, a bulk chloride concentration map (Fig. 7e) and its uncertainty map (Fig. 7f) are provided. The uncertainty in the precipitation mapping is neglected when chloride concentration uncertainty is calculated. The map (Fig. 7e) shows that bulk chloride concentration is about 5 mg/l in the centre of the MLR, increasing westward toward the coast and southeast-ward, to above 10 mg/l. The uncertainty in bulk chloride concentration is 1-1.5 mg/l for the central of the MLR, about 30% of estimated chloride concentration (Fig. 7f). This level of uncertainty is similar to that using much expensive $^{36}Cl/Cl$ method (Scanlon, 2000). However, due to the sparse sample points in the eastern part of the study area, the uncertainty is around and above 50% of the estimated chloride concentration. More sampling points are recommended for the future in this portion of the area.

4. Discussion

It is interesting to observe that elevation does not significantly influence chloride deposition, although it enhances precipitation in the study area. This result suggests either that chloride wet deposition does not increase proportionally with precipitation, or that the increase in wet deposition with elevation is compensated by a decrease in dry deposition with elevation, or both. Chloride concentration in instantaneous rain samples may give us some hint on how wet deposition is related to precipitation rate. A series of 1.6-mm rain samples were collected over a period with a single rainfall event (about 30 mm precipitation) on Flinders University campus on May 5th, 2008 (Fig. 8). It is observed that chloride concentration varies in a range between 3 and 17 mg/l. During the seven hour period, chloride concentration peaks at 9:00, 11:30, and 15:40. The subsequent rain samples after the peak time have lower chloride concentration. This indicates that the peak concentration samples were probably condensed earlier in the source cloud which dissolved more chloride-bearing aerosols, with the subsequent rain drops having less chloride aerosols to include. If we assume a similar mechanism applies to the whole area, it is easy to understand why wet deposition does not increase proportionally with precipitation. This is supported by the weak partial correlation between chloride deposition (D) and precipitation (P) when coastal distance (X) effect is removed (Fig. 4). Nevertheless, D is positively correlated (although not statistically significant, $r = 0.21$) to elevation (Z) when X effect is removed, suggesting elevation does weakly facilitate wet deposition, by increasing precipitation, but not in the same proportion to its effect on increasing precipitation. When X and P effect is removed, partial correlation between D and Z becomes negative. This result indicates that dry deposition slightly decreases with elevation. As elevation affects both wet and dry deposition in an opposite way, the chloride deposition becomes elevation-independent in the study area.

Another interesting finding is that chloride deposition in the east-facing slope is significantly larger than the west-facing slope when coastal distance effect is removed. Previously, we thought that the western slope, facing incoming chloride-bearing aerosols flux, might intercept atmospheric chloride and enhance deposition. This hypothesis is not supported by the correlation analysis results. As wind plays an important role in aerosol transport, analysis of wind direction may give us some hint. In Fig. 9, average sine values of wind direction at 09:00 a.m. (representing nigh-time wind) and 03:00 p.m. (representing daytime wind) are plotted against the longitude. The sine value is positive if the wind comes from the east, and negative if the wind comes from the west. During the day time, westerly winds dominate in the study area, which may facilitate aerosol transport to the east. When the westerly air mass is constrained by the topographic barrier on the western slope, windspeed increases, and reaches the maximum at the upwind side of the hill. The windspeed decreases over the downwind slope. This phenomenon has been extensively studied in sand dune formation processes (Andreotti et al., 2002). The elevated wind speed at the upwind slope facilitates atmospheric chloride transport, and a decreased wind speed at the downwind slope facilitates chloride deposition, which may explain the positive partial correlation between D and $\beta \sin \alpha$ from the data. The above discussion is based on that the ocean to the west of the study area is the only source of atmospheric chloride. Without further sampling and examination, other possibility cannot be excluded. For example, the positive partial correlation between D and $\beta \sin \alpha$ may be an artefact from local dust recycling. In the eastern flank of MLR, with dry climate, local dust may have higher chloride content than that in the western flank. If local dust brings some chloride to the BCD collectors, it may cause the difference between the two sides, leading to similar statistical association between D and $\beta \sin \alpha$.

5. Conclusions

Bulk chloride deposition in the Mount Lofty Ranges, a coastal hilly area in South Australia, was examined with selected geographical (easting and northing), orographic (elevation, slope and aspect), and atmospheric (precipitation) variables. Both partial correlation analysis and regression analysis were performed to understand the controlling factors in annual chloride deposition. The results indicate that the easting value of the site (equivalent to coastal distance), and terrain aspect and slope are two significant factors controlling chloride deposition. Coastal distance accounts for about 65% of the spatial variability in chloride deposition, with terrain aspect and slope accounting for about 8%. The deposition gradient is about 0.08 $gm^{-2}year^{-1}km^{-1}$ inland, within the range reported for other areas. The correlation results suggest that more chloride deposition occurs at the eastern slope than the western slope of MLR. The results also indicate that elevation slightly enhances wet deposition via increasing precipitation, but not in proportion to its effect on precipitation. Meanwhile, dry deposition is slightly weaker at higher elevations. These two opposite effects result in apparent elevation-independent chloride deposition in the study area.

Based on the regression analysis results, a published de-trended residual kriging mapping procedure (ASOADeK) was applied to construct the annual chloride deposition map and bulk chloride concentration map. The average uncertainty of the deposition map is about 20% in the western MLR, comparable to that of the $^{36}Cl/Cl$ method, and over 50% in the eastern MLR where more future sampling is recommended. The maps will be useful to examine catchment chloride balance for the CMB application in the study area, which will be the subject of a separate paper.

Acknowledgment

Constructive discussion with Graham Green and Erick Bestland is appreciated. The Department of Water, Land and Biodiversity Conservation of South Australia provided some precipitation chloride data, and GIS layers. Bureau of Meteorology provided long-term precipitation data, and wind speed data. Stacey Priestley (Flinders University), Darren Ray (BOM), Tania Wilson, Graham Green, and Eddie Banks (DWLBC) and Russell Jones (Water Data Services), assisted in data preparation.

References:

Alcala, F.J. and Custodio, E.: Atmospheric chloride deposition in continental Spain. Hydrol. Process., 22(18), 3636-3650, 2008a.

Alcala, F.J. and Custodio, E.: Using the Cl/Br ratio as a tracer to identify the origin of salinity in aquifers in Spain and Portugal. Journal of Hydrology, 359(1-2), 189-207, 2008b.

Andreotti, B., Claudin, P. and Douady, S.: Selection of dune shapes and velocities - Part 1: Dynamics of sand, wind and barchans. Eur. Phys. J. B, 28(3), 321-339, 2002.

Biggs, A.J.W.: Rainfall salt accessions in the Queensland Murray-Darling Basin. Australian Journal of Soil Research, 44(6), 637-645, 2006.

Blackburn, G. and McLeod, S.: Salinity of Atmospheric Precipitation in the Murray-Darling Drainage Division, Australia. Australian Journal of Soil Research, 21, 411-434, 1983.

BOM: Bureau of Meteorology of Australia, www.bom.gov.au, visited 2009.

Carratala, A., Gomez, A. and Bellot, J.: Mapping rain composition in the east of Spain by applying kriging. Water Air and Soil Pollution, 104(1-2), 9-27, 1998.

Contreras, S., Boer, M.M., Alcala, F.J., Domingo, F., Garcia, M., Pulido-Bosch, A. and Puigdefabregas, J.: An ecohydrological modelling approach for assessing long-term recharge rates in semiarid karstic landscapes. Journal of Hydrology, 351(1-2), 42-57, 2008.

Cook, P.G., Edmunds, W.M. and Gaye, C.B.: Estimating paleorecharge and paleoclimate from unsaturated zone profiles. Water Resour. Res., 28(10), 2721-2731, 1992.

Deutsch, C.V. and Journel, A.G.: GSLIB--Geostatistical Software Library and User's Guide. Applied Geostatistics Series. Oxford University Press, New York, 369 pp, 1998.

Dunn, S.M. and Bacon, J.R.: Assessing the value of Cl- and delta O-18 data in modelling the hydrological behaviour of a small upland catchment in northeast Scotland. Hydrol. Res., 39(5-6), 337-358, 2008.

Edmunds, W.M., Fellman, E., Goni, I.B. and Prudhomme, C.: Spatial and temporal distribution of groundwater recharge in northern Nigeria. Hydrogeol. J., 10(1), 205-215, 2002.

Eriksson, E.: The yearly circulation of chloride and sulphur in nature; meteorological, geochemical and pedological implications, part II. Tellus, 11(4), 375-403, 1959.

Eriksson, E.: The yearly circulation of chloride and sulphur in nature; meteorological, geochemical and pedological implications, part II. Tellus, 12, 63-109, 1960.

Eriksson, E. and Khunakasem, V.: Chloride concentrations in groundwater, recharge rate and rate of deposition of chloride in the Israel coastal plain. Journal of Hydrology, 7, 178-197, 1969.

Friedman, I., Smith, G.I., Gleason, J.D., Warden, A. and Harris, J.M.: Stable isotope composition of waters in southeastern California. 1. Modern precipitation. J. Geophys. Res.-Atmos., 97(D5), 5795-5812, 1992.

Goovaerts, P.: Geostatistical approaches for incorporating elevation into the spatial interpolation of rainfall. Journal of Hydrology, 228(1-2), 113-129, 2000.

Guan, H., Simmons, C.T. and Love, A.J.: Orographic controls on rain water isotope distribution in the Mount Lofty Ranges of South Australia. Journal of Hydrology, 374(3-4), 255-264, 2009.

Guan, H., Wilson, J.L. and Makhnin, O.: Geostatistical mapping of mountain precipitation incorporating autosearched effects of terrain and climatic characteristics. Journal of Hydrometeorology, 6(6), 1018-1031, 2005.

Gustafsson, M.E.R. and Larsson, E.H.: Spatial and temporal patterns of chloride deposition in Southern Sweden. Water Air and Soil Pollution, 124(3-4), 345-369, 2000.

Hrachowitz, M., Soulsby, C., Tetzlaff, D., Dawson, J.J.C. and Malcolm, I.A.: Regionalization of transit time estimates in montane catchments by integrating landscape controls. Water Resour. Res., 45, 18, 2009.

Isaaks, E.H. and Srivastava, R.M.: Applied Geostatistics. Oxford Unviersity Press, Inc, 561 pp, 1989.

Kayaalp, A.S.: Application of rainfall chemistry and isotope data to hydro-meteorological modelling. Ph.D. Thesis, Flinders University, Adelaide, Australia, 273 pp, 2001.

Keywood, M.D., Chivas, A.R., Fifield, L.K., Cresswell, R.G. and Ayers, G.P.: The accession of chloride to the western half of the Australian continent. Australian Journal of Soil Research, 35(5), 1177-1189, 1997.

Kirchner, J.W., Feng, X.H. and Neal, C.: Fractal stream chemistry and its implications for contaminant transport in catchments. Nature, 403(6769), 524-527, 2000.

Lewis, E.R. and Schwartz, S.E.: Sea Salt Aerosol Production: Mechanisms, Methods, Measurements and Models -- A Critical Review. Geophysical Monograph 152. American Geophysical Union, Washington, DC, 413 pp, 2004.

Lowry, R.: Concepts and Applications of Inferential Statistics. http://faculty.vassar.edu/lowry/webtext.html, Vassar College, Poughkeepsie, NY USA,1999-2009.

Minor, T.B., Russell, C.E. and Mizell, S.A.: Development of a GIS-based model for extrapolating mesoscale groundwater recharge estimates using integrated geospatial data sets. Hydrogeol. J., 15(1), 183-195, 2007.

Moreno, G., Gallardo, J.F. and Bussotti: Canopy modification of atmospheric deposition in oligotrophic Quercus pyrenaica forests of an unpolluted region (central-western Spain). For. Ecol. Manage., 149(1-3), 47-60, 2001.

Phillips, F.M.: Environmental tracers for water movement in desert soils of the American southwest. Soil Sci. Soc. Am. J., 58(1), 15-24, 1994.

Preiss, W.V.: The Adelaide Geosyncline: Late proterozoic stratigraphy, sedimentation, palaeontology and tectonics. Bulletin / Geological Survey of South Australia, 53, 439, 1987.

Scanlon, B.R.: Uncertainties in estimating water fluxes and residence times using environmental tracers in an arid unsaturated zone. Water Resour. Res., 36(2), 395-409, 2000.

Scanlon, B.R., Healy, R.W. and Cook, P.G.: Choosing appropriate techniques for quantifying groundwater recharge. Hydrogeol. J., 10(1), 18-39, 2002.

Shaw, S.B., Harpold, A.A., Taylor, J.C. and Walter, M.T.: Investigating a high resolution, stream chloride time series from the Biscuit Brook catchment, Catskills, NY. Journal of Hydrology, 348(3-4), 245-256, 2008.

Walker, G.R., Jolly, I.D. and Cook, P.G.: A new chloride leaching approach to the estimation of diffuse recharge following a change in land use. Journal of Hydrology, 128, 49-67, 1991.

Wilson, J.L. and Guan, H.: Mountain-block hydrology and mountain-front recharge. In: J.F. Hogan, F.M. Phillips and B.R. Scanlon (Editors), Groundwater Recharge in a Desert Environment: The Southwestern United States. Water Science and Applications Series. American Geophysical Union, Washington, D.C., pp. 113-137, 2004.

Wood, W.W. and Sanford, W.E.: Chemical and isotopic methods for quantifying groundwater recharge in a regional, semiarid environment. Ground Water, 33(3), 458-468, 1995.

Figure captions:

Figure 1 The DEM map of the study area with 17 sampling sites (crossed circles) of bulk chloride, with insert maps of Australia and South Australia showing the regional location of the study area, and an insert map of annual precipitation overlain by 41 wind observation sites (stars). The numbers next to the chloride sites correspond to those in Table 1. The Bureau of Meteorology IDs of the four selected wind sites from northwest to southeast are 23090 (W1), 23733 (W2), 23842 (W3), and 24545 (W4). The longitude and latitude marks are for the DEM map.

Figure 2 Histograms of wind direction observed at 9:00AM (left column) and 3:00PM (right column) for four selected wind observation sites (W1, W2, W3, and W4 in Figure 1). Horizontal axis shows bin centres of the wind direction in degree clockwise from the north. The data were collected by BOM in 1977-2008, 1957-2008, 1987-2008, and 1965-1969 for the four sites, respectively.

Figure 3 Annual chloride deposition vs. UTM Easting (as a proxy for coastal distance), with sites #16 and #17 excluded). The numbers next to the symbols correspond to those in Table 1 and Figure 1.

Figure 4 (Partial) correlation coefficient between yearly chloride deposition and each of the selected variables, with or without the effects of other variables (specified in the bracket) removed. The dash line is 90% significance for easy comparison between correlations.

Figure 5 Calculated semivariograms with a 10-km lag separation distance, and a 2-km lag tolerance, and the model fitting for (a) one cross validation set of observed annual mean chloride deposition, and (b) regression de-trended residuals over the 17 sites. The fitted model is a Gaussian model (range = 48 km, sill = 1.8 $(gm^{-2})^2$, and nugget = 0.05 $(gm^{-2})^2$) for (a), and a spherical model (range = 40 km, sill = 0.29 $(gm^{-2})^2$, and nugget = 0.2 $(gm^{-2})^2$) for (b).

Figure 6 (a) Cross-validation estimates of regression, ASOADeK, and direct ordinary kriging, and (b) regression estimates of annual chloride deposition (for the 15 sites) and ASOADeK estimates (for all 17 sites), in comparison to the observations. The MAE values are mean absolute errors (g/m^2) of the observation sites, and the *r* values are Pearson correlation coefficients between the estimates and the observations.

Figure 7 Various mapping results of annual chloride deposition and related quantities over the study area: (a) regression map, (b) residual kriging map, (c) ASOADeK map, (d) ASOADeK map uncertainty, (e) bulk chloride concentration map, and (f) concentration map uncertainty. The uncertainty is estimated at 90% confidence level. The cross symbols on (d) is the bulk chloride sampling sites (Figure 1). The missing data in the southwest corner on the maps of b through f is because the residual kriging does not produce reasonable estimates due to lack of data over this part of the area.

Figure 8 Chloride concentration in each of the sequential 1.6 mm rain samples collected at Flinders University campus on 16/5/2008.

Figure 9 Mean values of *sin(wind direction)* at the 41 observation sites (Figure 1) for two seasons: (a) summer months (12, 1, 2), and (b) winter months (6, 7, 8).

Table 1. Bulk chloride deposition and concentration over the Mount Lofty Ranges calculated from samples collected over two periods by DWLBC (1-8) and Flinders University (9-17), and associated site information

ID	Site id	Site name	Easting (m)	Northing (m)	Elevation[1] (m)	Aspect (°)	Slope (°)	Precip.[2] (mm)	Data period m/y-m/y	Concentration[3] (mg/l)	Deposition (g/m^2/yr)
1	AW503502	Scott Creek	287895	6113235	272	246	0.09	751	02/03-02/05	5.4	4.05
2	AW426638	Mount Barker	306288	6117246	323	121	0.06	705	11/02-11/04	6.1	4.63
3	AW504512	Mt Pleasant	319631	6148870	425	132	0.03	731	12/02-10/03	5.2	2.57
4	AW504559	Cherryville	295316	6134505	531	303	0.15	1000	01/03-07/03	4.2	4.37
5	AW504563	Milbrook	300896	6143374	328	310	0.08	728	07/03-03/04	5.9	3.65
6	AW505517	Penrice	321661	6184765	314	296	0.06	557	12/03-11/04	4.1	1.98
7	AW505537	Mount Adam	318897	6165439	515	50	0.00	868	11/02-11/04	4.1	3.32
8	AW505500	Warren Reservoir	309409	6157186	391	290	0.10	778	10/03-11/04	4.8	3.99
9	Kyp02	Hallett Cove	273701	6115600	125	281	0.13	654	04/92-12/94	12.2	6.97
10	Kyp03	Bedford Park	278584	6121170	161	291	0.17	638	04/92-12/94	6.0	3.97
11	Kyp04	Happy Valley	279315	6115516	149	274	0.15	692	06/92-11/94	4.9	3.78
12	Kyp05	Flagstaff Hill	279991	6118507	180	282	0.17	714	06/92-12/94	6.5	5.10
13	Kyp06	Heathfield	292858	6120585	414	220	0.07	983	07/92-12/94	4.7	4.76
14	Kyp07	Hahndorf	300232	6121471	340	155	0.05	796	07/92-12/94	5.1	4.67
15	Kyp08	Mannum	345887	6135339	47	155	0.02	280	06/92-12/94	3.7	1.33
16	Kyp09	Murray Bridge	342703	6112274	9	104	0.03	340	06/92-12/94	6.1	2.54
17	Kyp10	Tailem Bend	359324	6097715	12	214	0.02	430	07/92-12/94	5.7	2.59

1. The elevation is 1-km pixel elevation, while aspect and slope are 7-km pixel values optimized in the regression.
2. Precipitation is annual precipitation estimated based on long-term observations (Guan et al., 2009).
3. This is weight mean bulk chloride concentration.

Table 2 Correlation matrix of chloride deposition and selected variables for sites #1-15 (P is long-term mean annual precipitation, other symbols are described in Eq. (4), the correlation coefficients in bold face are significant at 90% confidence level).

	D	*P*	*X*	*Y*	*Z*	βcos(α)	βsin(α)
D	1						
P	**0.48**	1					
X	**-0.81**	**-0.41**	1				
Y	**-0.61**	-0.09	**0.65**	1			
Z	-0.03	**0.79**	0.19	**0.44**	1		
βcos(α)	0.09	0.05	-0.28	0.22	0.01	1	
βsin(α)	**-0.41**	-0.12	**0.74**	0.29	0.32	**-0.67**	1

Table 3 Regression results of chloride deposition with *X*, *X* and *βsinα*, respectively, based on observations of sites 1-15 (the 15-site average mean annual chloride deposition is 3.94 g/m^2)

Predictor variables		b_0	b_1X	$b_5\beta\sin\alpha$	R^2	Adjusted[a] R^2	MAE[b]
X	coefficients	9.40	-0.054		0.65	0.62	0.63
	p values	1E-06	3E-04				
X, βsinα	coefficients	11.95	-0.075	7.72	0.73	0.68	0.54
	p values	0.0000	0.0003	0.090			

a. Adjusted coefficient of multiple determination considering the number of predictor variables effect.
b. MAE is the regression mean absolute error (g/m^2).

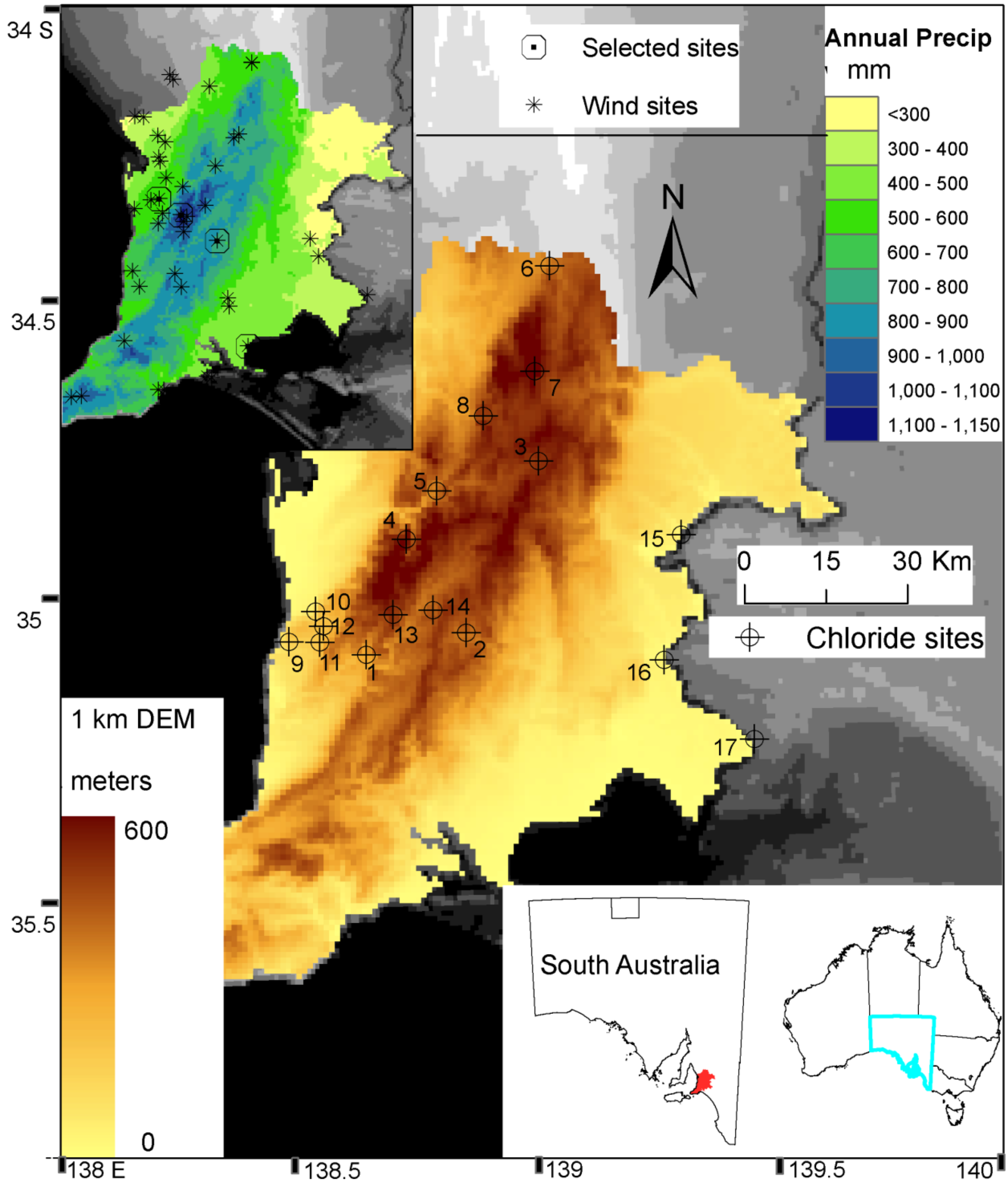

Figure 1 The DEM map of the study area with 17 sampling sites (crossed circles) of bulk chloride, with insert maps of Australia and South Australia showing the regional location of the study area, and an insert map of annual precipitation overlain by 41 wind observation sites (stars). The numbers next to the chloride sites correspond to those in Table 1. The Bureau of Meteorology IDs of the four selected wind sites from northwest to southeast are 23090 (W1), 23733 (W2), 23842 (W3), and 24545 (W4). The longitude and latitude marks are for the DEM map.

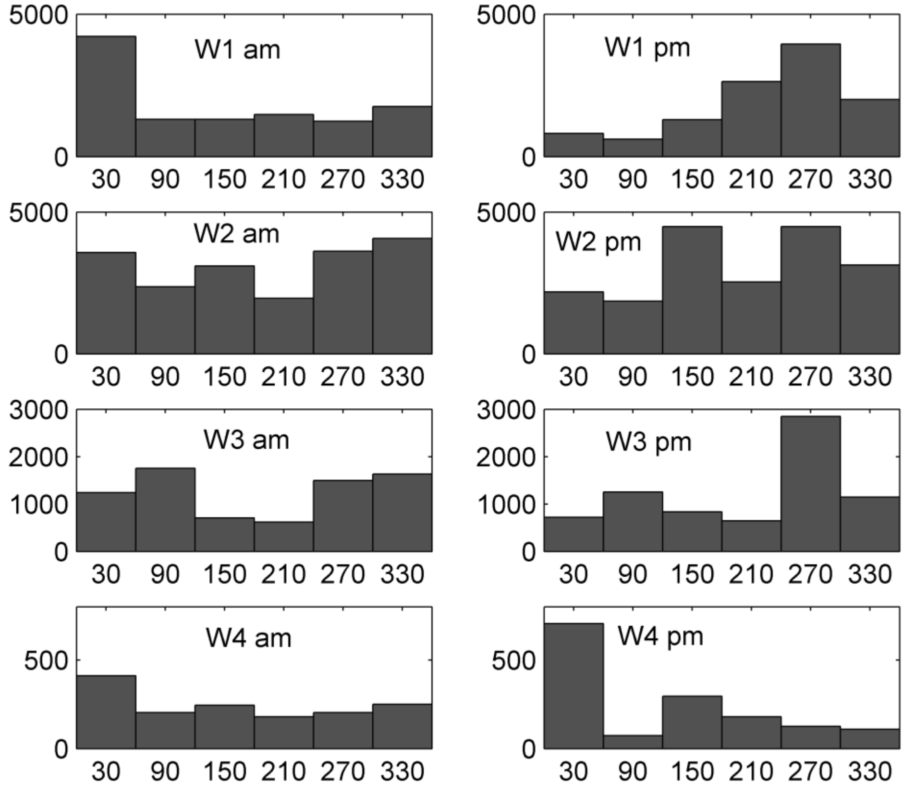

Figure 2 Histograms of wind direction observed at 9:00AM (left column) and 3:00PM (right column) for four selected wind observation sites (W1, W2, W3, and W4 in Figure 1). Horizontal axis shows bin centres of the wind direction in degree clockwise from the north. The data were collected by BOM in 1977-2008, 1957-2008, 1987-2008, and 1965-1969 for the four sites, respectively.

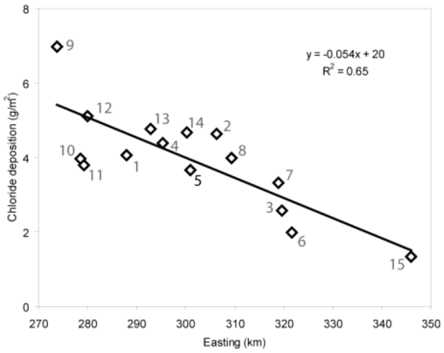

Figure 3 Annual chloride deposition vs. UTM Easting (as a proxy for coastal distance), with sites #16 and #17 excluded). The numbers next to the symbols correspond to those in Table 1 and Figure 1.

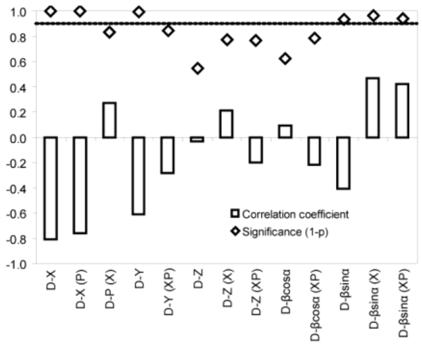

Figure 4 (Partial) correlation coefficient between yearly chloride deposition and each of the selected variables, with or without the effects of other variables (specified in the bracket) removed. The dash line is 90% significance for easy comparison between correlations.

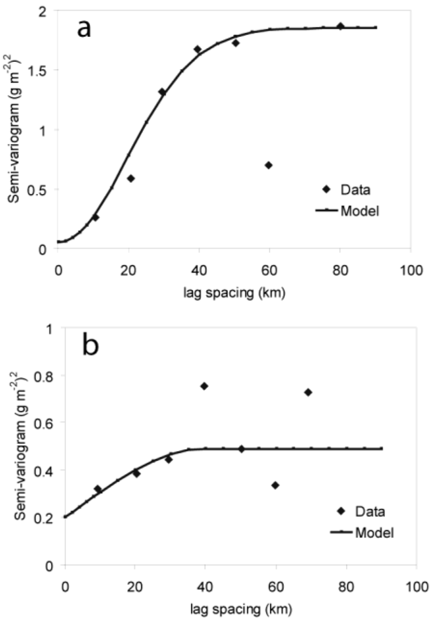

Figure 5 Calculated semivariograms with a 10-km lag separation distance, and a 2-km lag tolerance, and the model fitting for (a) one cross validation set of observed annual mean chloride deposition, and (b) regression de-trended residuals over the 17 sites. The fitted model is a Gaussian model (range = 48 km, sill = 1.8 $(gm^{-2})^2$, and nugget = 0.05 $(gm^{-2})^2$) for (a), and a spherical model (range = 40 km, sill = 0.29 $(gm^{-2})^2$, and nugget = 0.2 $(gm^{-2})^2$) for (b).

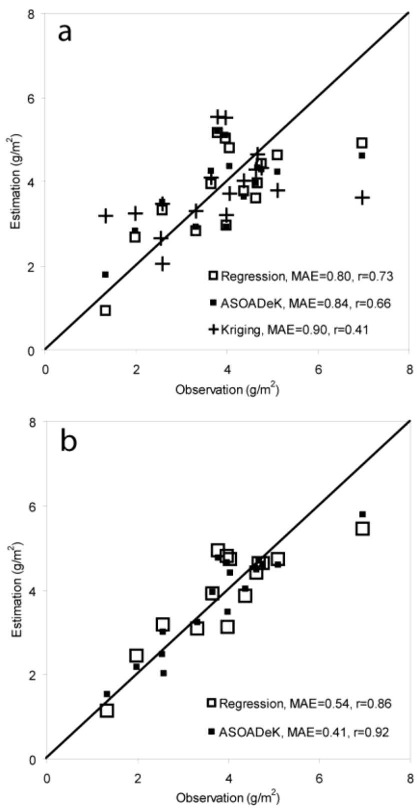

Figure 6 (a) Cross-validation estimates of regression, ASOADeK, and direct ordinary kriging, and (b) regression estimates of annual chloride deposition (for the 15 sites) and ASOADeK estimates (for all 17 sites), in comparison to the observations. The MAE values are mean absolute errors (g/m^2) of the observation sites, and the *r* values are Pearson correlation coefficients between the estimates and the observations.

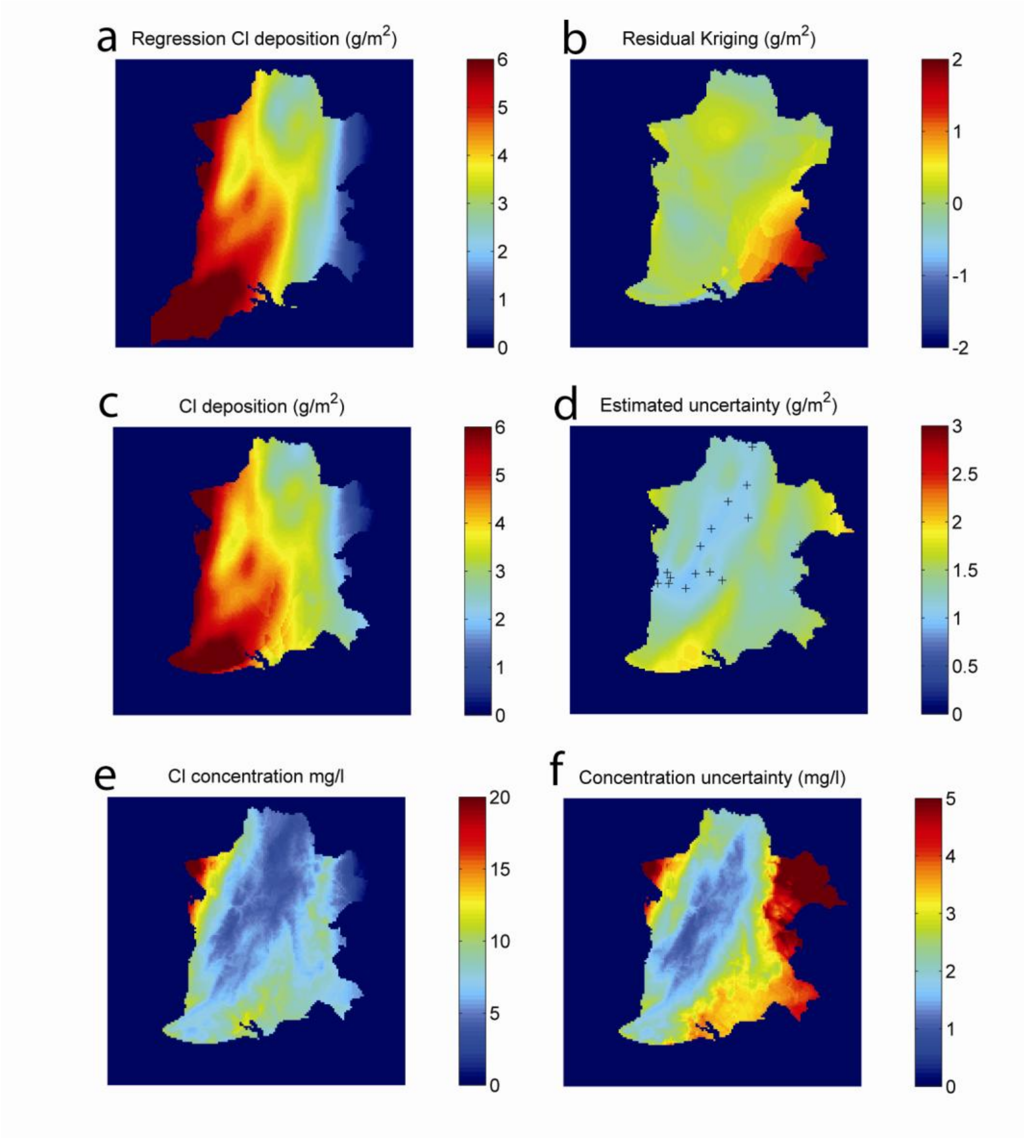

Figure 7 Various mapping results of annual chloride deposition and related quantities over the study area: (a) regression map, (b) residual kriging map, (c) ASOADeK map, (d) ASOADeK map uncertainty, (e) bulk chloride concentration map, and (f) concentration map uncertainty. The uncertainty is estimated at 90% confidence level. The cross symbols on (d) is the bulk chloride sampling sites (Figure 1). The missing data in the southwest corner on the maps of b through f is because the residual kriging does not produce reasonable estimates due to lack of data over this part of the area.

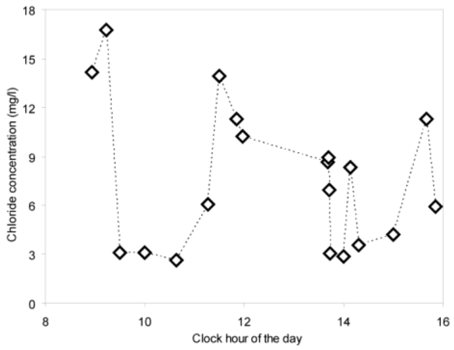

Figure 8 Chloride concentration in each of the sequential 1.6 mm rain samples collected at Flinders University campus on 16/5/2008.

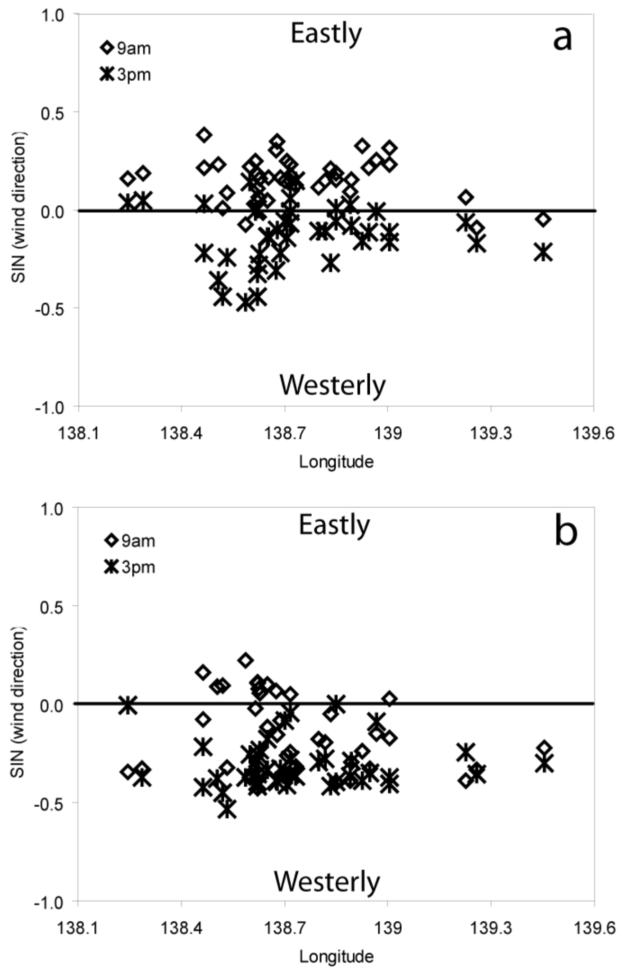

Figure 9 Mean values of *sin(wind direction)* at the 41 observation sites (Figure 1) for two seasons: (a) summer months (12, 1, 2), and (b) winter months (6, 7, 8).